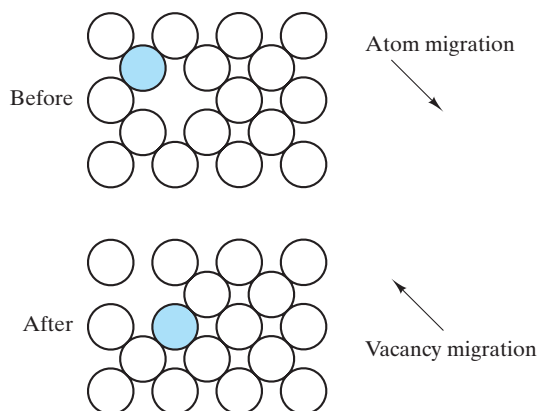


### 5.3 Point Defects and Solid-State Diffusion

At sufficient temperatures, atoms and molecules can be quite mobile in both liquids and solids. Watching a drop of ink fall into a beaker of water and spread out until all the water is evenly colored gives a simple demonstration of **diffusion**, the movement of molecules from an area of higher concentration to an area of lower concentration. But diffusion is not restricted to different materials. At room temperature, H<sub>2</sub>O molecules in pure water are in continuous motion and are migrating through the liquid as an example of **self-diffusion**. This atomic-scale motion is relatively rapid in liquids and relatively easy to visualize. It is more difficult to visualize diffusion in rigid solids. Nonetheless, diffusion does occur in the solid state. A primary difference between solid-state and liquid-state diffusion is the low rate of diffusion in solids. Looking back at the crystal structures of Chapter 3, we can appreciate that diffusion of atoms or ions through those generally tight structures is difficult. In fact, the energy requirements to squeeze most atoms or ions through perfect crystal structures are so high as to make diffusion nearly impossible. To make solid-state diffusion practical, point defects are generally required. Figure 5.5 illustrates how atomic migration becomes possible without major crystal-structure distortion by means of a **vacancy migration** mechanism. It is important to note that the overall direction of material flow is opposite to the direction of vacancy flow.

Figure 5.6 shows diffusion by an interstitialcy mechanism and illustrates effectively the **random-walk** nature of atomic migration. This randomness does not preclude the net flow of material when there is an overall variation in chemical composition. This frequently occurring case is illustrated in Figures 5.7 and 5.8. Although each atom of solid A has an equal probability of randomly “walking” in any direction, the higher initial concentration of A on the left side of the system will cause such random motion to produce *interdiffusion*, a net flow of A atoms into solid B. Similarly, solid B diffuses into solid A. The formal



**FIGURE 5.5** Atomic migration occurs by a mechanism of vacancy migration. Note that the overall direction of material flow (the atom) is opposite to the direction of vacancy flow.

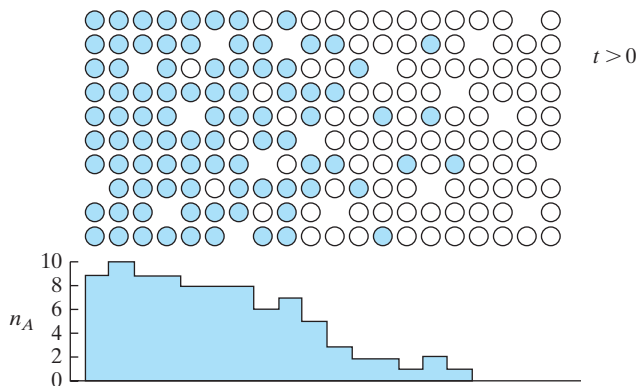
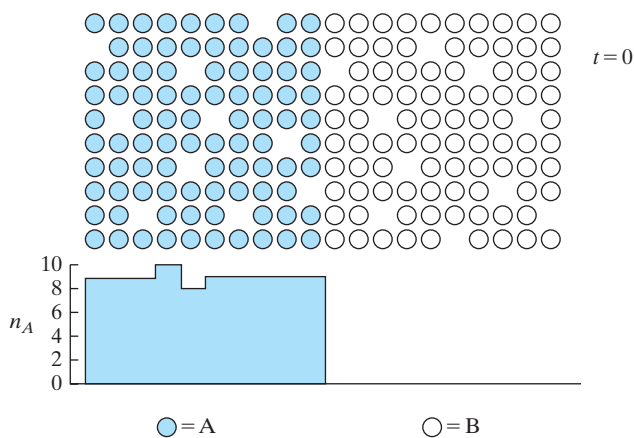


**FIGURE 5.7** The interdiffusion of materials A and B. Although any given A or B atom is equally likely to “walk” in any random direction (see Figure 5.6), the concentration gradients of the two materials can result in a net flow of A atoms into the B material, and vice versa.

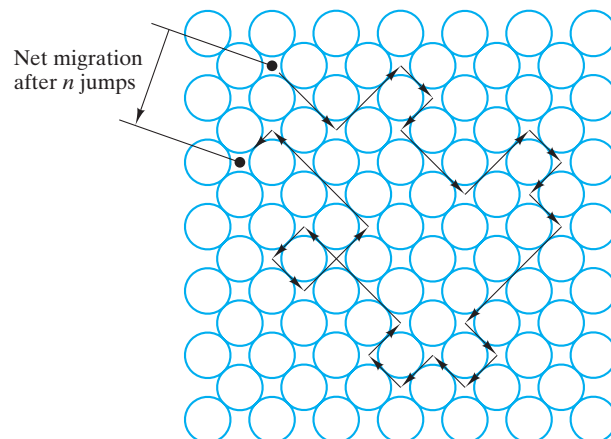


**FIGURE 5.6** Diffusion by an interstitialcy mechanism illustrating the random-walk nature of atomic migration.



The schematic illustrations on this page show how the atomic scale defects of Figure 4.8 facilitate diffusion. The application of these mechanisms in various heat treatments will be seen in Chapter 10.

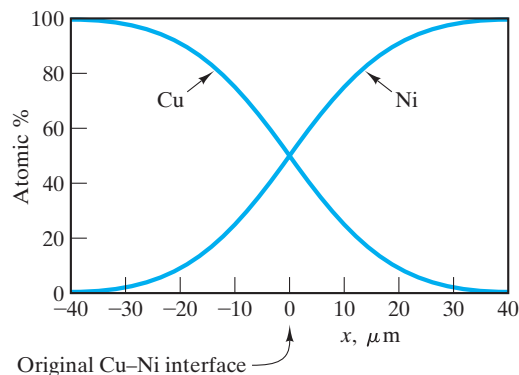


**FIGURE 5.8** The interdiffusion of materials on an atomic scale was illustrated in Figure 5.7. This interdiffusion of copper and nickel is a comparable example on the microscopic scale.

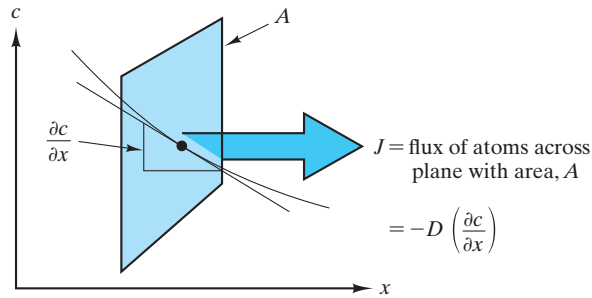


FIGURE 5.9 Geometry of Fick's first law (Equation 5.8).

mathematical treatment of such a diffusional flow begins with an expression known as **Fick's\* first law**,

$$J_x = -D \frac{\partial c}{\partial x}, \quad (5.8)$$

where  $J_x$  is the *flux*, or flow rate, of the diffusing species in the  $x$ -direction due to a **concentration gradient** ( $\partial c / \partial x$ ). The proportionality coefficient,  $D$ , is called the **diffusion coefficient** or, simply, the **diffusivity**. The geometry of Equation 5.8 is illustrated in Figure 5.9. Figure 5.7 reminds us that the concentration gradient at a specific point along the diffusion path changes with time,  $t$ . This transient condition is represented by a second-order differential equation also known as **Fick's second law**,

$$\frac{\partial c_x}{\partial t} = \frac{\partial}{\partial x} \left( D \frac{\partial c_x}{\partial x} \right). \quad (5.9)$$

For many practical problems, one can assume that  $D$  is independent of  $c$ , leading to a simplified version of Equation 5.9:

$$\frac{\partial c_x}{\partial t} = D \frac{\partial^2 c_x}{\partial x^2}. \quad (5.10)$$

Figure 5.10 illustrates a common application of Equation 5.10, the diffusion of material into a semi-infinite solid while the surface concentration of the diffusing species,  $c_s$ , remains constant. Two examples of this system would be the plating of metals and the saturation of materials with reactive atmospheric gases. Specifically, steel surfaces are often hardened by **carburization**, the diffusion of carbon atoms into the steel from a carbon-rich environment. The solution to this differential equation with the given boundary conditions is

$$\frac{c_x - c_0}{c_s - c_0} = 1 - \operatorname{erf} \left( \frac{x}{2\sqrt{Dt}} \right), \quad (5.11)$$

\*Adolf Eugen Fick (1829–1901), German physiologist. The medical sciences frequently apply principles previously developed in the fields of mathematics, physics, and chemistry. However, Fick's work in the "mechanistic" school of physiology was so excellent that it served as a guide for the physical sciences. He developed the diffusion laws as part of a study of blood flow.

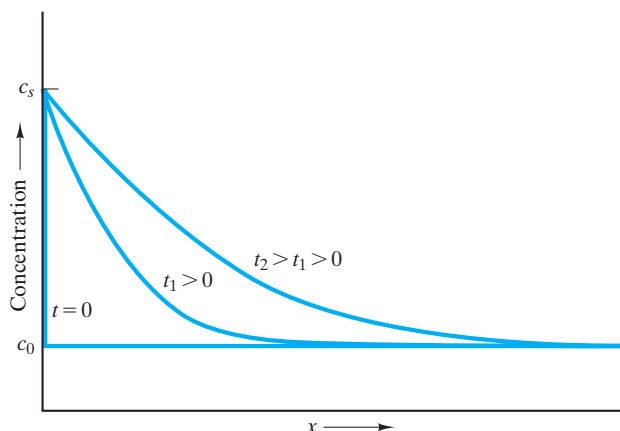


**FIGURE 5.10** Solution to Fick's second law (Equation 5.10) for the case of a semi-infinite solid, constant surface concentration of the diffusing species  $c_s$ , initial bulk concentration  $c_0$ , and a constant diffusion coefficient,  $D$ .

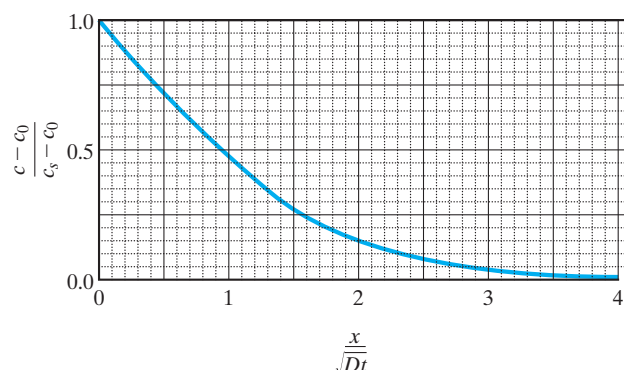


**FIGURE 5.11** Master plot summarizing all of the diffusion results of Figure 5.10 on a single curve.

where  $c_0$  is the initial bulk concentration of the diffusing species and erf refers to the **Gaussian\* error function**, based on the integration of the “bell-shaped” curve with values readily available in mathematical tables. Representative values are given in Table 5.1. A great power of this analysis is that the result (Equation 5.11) allows all of the concentration profiles of Figure 5.10 to be redrawn on a single master plot (Figure 5.11). Such a plot permits rapid calculation of the time necessary for relative saturation of the solid as a function of  $x$ ,  $D$ , and  $t$ .

The preceding mathematical analysis of diffusion implicitly assumed a fixed temperature. Our previous discussion of the dependence of diffusion on point defects causes us to expect a strong temperature dependence for diffusivity by analogy to Equation 5.5—and this is precisely the case. Diffusivity data are perhaps the best known examples of an Arrhenius equation

$$D = D_0 e^{-q/kT}, \quad (5.12)$$

where  $D_0$  is the preexponential constant and  $q$  is the activation energy for defect motion. In general,  $q$  is not equal to the  $E_{\text{defect}}$  of Equation 5.5.  $E_{\text{defect}}$  represents the energy required for defect formation, while  $q$  represents the energy required for the movement of that defect through the crystal structure ( $E_{\text{defect motion}}$ ) for *interstitial diffusion*. For the vacancy mechanism, vacancy formation is an integral part of the diffusional process (see Figure 5.5), and  $q = E_{\text{defect}} + E_{\text{defect motion}}$ .

\*Johann Karl Friedrich Gauss (1777–1855), German mathematician, was one of the great geniuses in the history of mathematics. In his teens, he developed the method of least squares for curve-fitting data. Much of his work in mathematics was similarly applied to physical problems, such as astronomy and geomagnetism. His contribution to the study of magnetism led to the unit of magnetic-flux density being named in his honor.

TABLE 5.1

The Error Function			
$z$	$\text{erf}(z)$	$z$	$\text{erf}(z)$
0.00	0.0000	0.70	0.6778
0.01	0.0113	0.75	0.7112
0.02	0.0226	0.80	0.7421
0.03	0.0338	0.85	0.7707
0.04	0.0451	0.90	0.7969
0.05	0.0564	0.95	0.8209
0.10	0.1125	1.00	0.8427
0.15	0.1680	1.10	0.8802
0.20	0.2227	1.20	0.9103
0.25	0.2763	1.30	0.9340
0.30	0.3286	1.40	0.9523
0.35	0.3794	1.50	0.9661
0.40	0.4284	1.60	0.9763
0.45	0.4755	1.70	0.9838
0.50	0.5205	1.80	0.9891
0.55	0.5633	1.90	0.9928
0.60	0.6039	2.00	0.9953
0.65	0.6420		

Source: *Handbook of Mathematical Functions*, M. Abramowitz and I. A. Stegun, Eds., National Bureau of Standards, Applied Mathematics Series 55, Washington, DC, 1972.

It is more common to tabulate diffusivity data in terms of molar quantities (i.e., with an activation energy,  $Q$ , per mole of diffusing species),

$$D = D_0 e^{-Q/RT}, \quad (5.13)$$

where  $R$  is the universal gas constant ( $= N_{\text{AV}}k$ ), as discussed previously. Figure 5.12 shows an Arrhenius plot of the diffusivity of carbon in  $\alpha$ -Fe over a range of temperatures, which is an example of an interstitial mechanism as sketched in Figure 5.6. Figure 5.13 collects diffusivity data for a number of metallic systems. Table 5.2 gives the Arrhenius parameters for these data. It is useful to compare different data sets. For instance, C can diffuse by an interstitial mechanism through bcc Fe more readily than through fcc Fe ( $Q_{\text{bcc}} < Q_{\text{fcc}}$  in Table 5.2). The greater openness of the bcc structure (Section 3.2) makes this difference understandable. Similarly, the self-diffusion of Fe by a vacancy mechanism is greater in bcc Fe than in fcc Fe. Figure 5.14 and Table 5.3 give comparable diffusivity data for several nonmetallic systems. In many compounds, such as  $\text{Al}_2\text{O}_3$ , the smaller ionic species (e.g.,  $\text{Al}^{3+}$ ) diffuse much more readily through the system. The Arrhenius behavior of ionic diffusion in ceramic compounds is especially analogous to the temperature dependence of semiconductors to be discussed in Chapter 13. It is this ionic transport mechanism that is responsible for the semiconducting behavior of certain ceramics such as ZnO; that is, charged ions rather than electrons produce the measured electrical conductivity. Polymer data are not included with the other nonmetallic systems of Figure 5.14 and Table 5.3 because most commercially important diffusion mechanisms in polymers involve the liquid state or the amorphous solid state, where the point-defect mechanisms of this section do not apply.

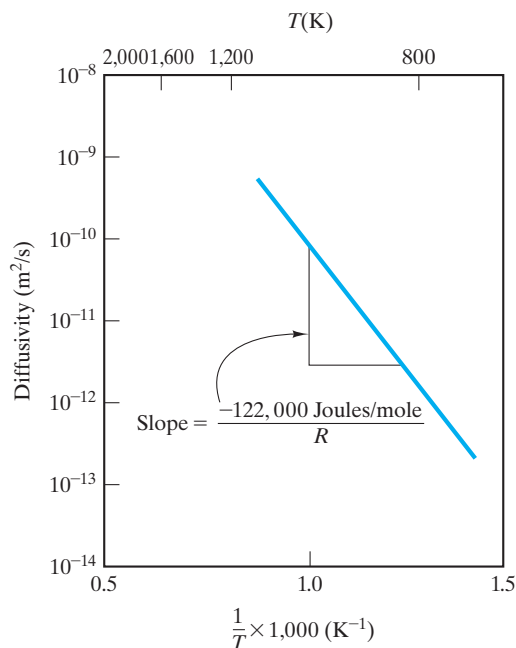


**FIGURE 5.12** Arrhenius plot of the diffusivity of carbon in  $\alpha$ -iron over a range of temperatures. Note also related Figures 4.4 and 5.6 and other metallic diffusion data in Figure 5.13.

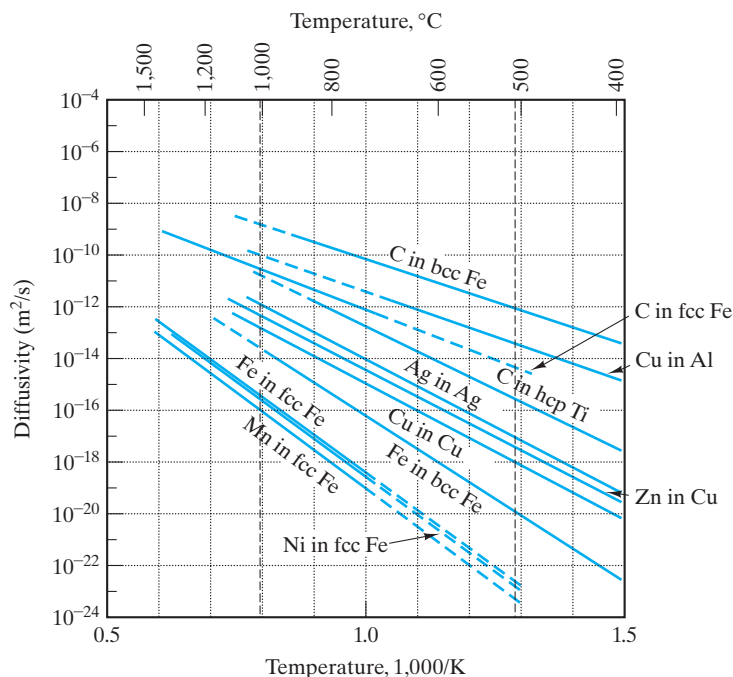


**FIGURE 5.13** Arrhenius plot of diffusivity data for a number of metallic systems. (From L. H. Van Vlack, *Elements of Materials Science and Engineering*, 4th ed., Addison-Wesley Publishing Co., Inc., Reading, MA, 1980.)

**TABLE 5.2**

Diffusivity Data for a Number of Metallic Systems<sup>a</sup>

Solute	Solvent	$D_0$ (m <sup>2</sup> /s)	$Q$ (kJ/mol)	$Q$ (kcal/mol)
Carbon	Fcc iron	$20 \times 10^{-6}$	142	34.0
Carbon	Bcc iron	$220 \times 10^{-6}$	122	29.3
Iron	Fcc iron	$22 \times 10^{-6}$	268	64.0
Iron	Bcc iron	$200 \times 10^{-6}$	240	57.5
Nickel	Fcc iron	$77 \times 10^{-6}$	280	67.0
Manganese	Fcc iron	$35 \times 10^{-6}$	282	67.5
Zinc	Copper	$34 \times 10^{-6}$	191	45.6
Copper	Aluminum	$15 \times 10^{-6}$	126	30.2
Copper	Copper	$20 \times 10^{-6}$	197	47.1
Silver	Silver	$40 \times 10^{-6}$	184	44.1
Carbon	Hcp titanium	$511 \times 10^{-6}$	182	43.5

<sup>a</sup>See Equation 5.13.

Source: Data from L. H. Van Vlack, *Elements of Materials Science and Engineering*, 4th ed., Addison-Wesley Publishing Co., Inc., Reading, MA, 1980.

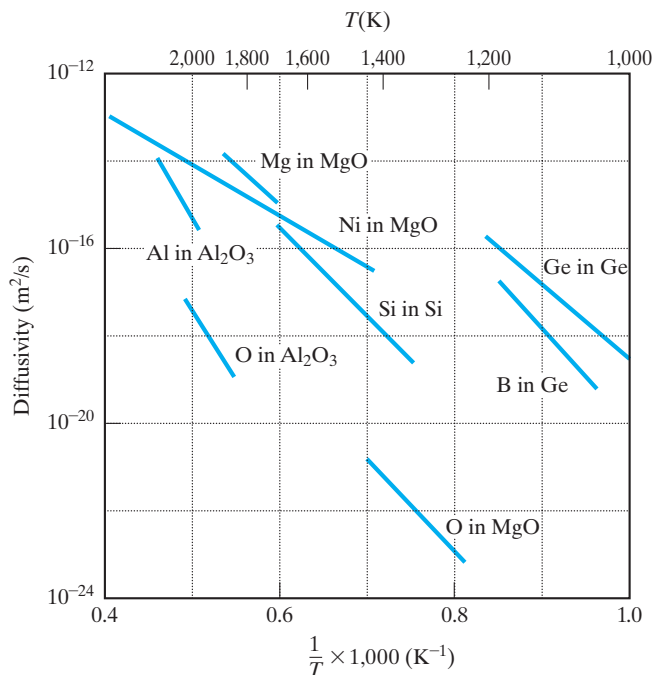


**FIGURE 5.14** Arrhenius plot of diffusivity data for a number of nonmetallic systems. (From P. Kofstad, *Nonstoichiometry, Diffusion, and Electrical Conductivity in Binary Metal Oxides*, John Wiley & Sons, Inc., NY, 1972; and S. M. Hu in *Atomic Diffusion in Semiconductors*, D. Shaw, Ed., Plenum Press, New York, 1973.)

**TABLE 5.3**

**Diffusivity Data for a Number of Nonmetallic Systems<sup>a</sup>**

Solute	Solvent	$D_0(\text{m}^2/\text{s})$	$Q(\text{kJ/mol})$	$Q(\text{kcal/mol})$
Al	$\text{Al}_2\text{O}_3$	$2.8 \times 10^{-3}$	477	114.0
O	$\text{Al}_2\text{O}_3$	0.19	636	152.0
Mg	MgO	$24.9 \times 10^{-6}$	330	79.0
O	MgO	$4.3 \times 10^{-9}$	344	82.1
Ni	MgO	$1.8 \times 10^{-9}$	202	48.3
Si	Si	0.18	460	110.0
Ge	Ge	$1.08 \times 10^{-3}$	291	69.6
B	Ge	$1.1 \times 10^3$	439	105.0

<sup>a</sup>See Equation 5.13.

Source: Data from P. Kofstad, *Nonstoichiometry, Diffusion, and Electrical Conductivity in Binary Metal Oxides*, John Wiley & Sons, Inc., New York, 1972; and S. M. Hu, in *Atomic Diffusion in Semiconductors*, D. Shaw, Ed., Plenum Press, New York, 1973.

**EXAMPLE 5.3**

Steel surfaces can be hardened by *carburization*, as discussed relative to Figure 5.10. During one such treatment at 1,000°C, there is a drop in carbon concentration from 5 to 4 at % carbon between 1 and 2 mm from the surface of the steel. Estimate the flux of carbon atoms into the steel in this near-surface region. (The density of  $\gamma$ -Fe at 1,000°C is 7.63 g/cm<sup>3</sup>.)

**SOLUTION**

First, we approximate

$$\begin{aligned}\frac{\partial c}{\partial x} &\simeq \frac{\Delta c}{\Delta x} = \frac{5 \text{ at \%} - 4 \text{ at \%}}{1 \text{ mm} - 2 \text{ mm}} \\ &= -1 \text{ at \% / mm.}\end{aligned}$$

To obtain an absolute value for carbon-atom concentration, we must first know the concentration of iron atoms. From the given data and Appendix 1,

$$\rho = 7.63 \frac{\text{g}}{\text{cm}^3} \times \frac{0.6023 \times 10^{24} \text{ atoms}}{55.85 \text{ g}} = 8.23 \times 10^{22} \frac{\text{atoms}}{\text{cm}^3}.$$

Therefore,

$$\begin{aligned}\frac{\Delta c}{\Delta x} &= -\frac{0.01(8.23 \times 10^{22} \text{ atoms/cm}^3)}{1 \text{ mm}} \times \frac{10^6 \text{ cm}^3}{\text{m}^3} \times \frac{10^3 \text{ mm}}{\text{m}} \\ &= -8.23 \times 10^{29} \text{ atoms/m}^4.\end{aligned}$$

From Table 5.2,

$$\begin{aligned}D_c \text{ in } \gamma - \text{Fe, } 1000^\circ\text{C} &= D_0 e^{-Q/RT} \\ &= (20 \times 10^{-6} \text{ m}^2/\text{s}) e^{-(142,000 \text{ J/mol})/(8.314 \text{ J/mol/K})(1273 \text{ K})} \\ &= 2.98 \times 10^{-11} \text{ m}^2/\text{s}.\end{aligned}$$

Using Equation 5.8 gives us

$$\begin{aligned}J_x &= -D \frac{\partial c}{\partial x} \\ &\simeq -D \frac{\Delta c}{\Delta x} \\ &= -(2.98 \times 10^{-11} \text{ m}^2/\text{s})(-8.23 \times 10^{29} \text{ atoms/m}^4) \\ &= 2.45 \times 10^{19} \text{ atoms}/(\text{m}^2 \cdot \text{s})\end{aligned}$$

**EXAMPLE 5.4**

The diffusion result described by Equation 5.11 can apply to the carburization process (Example 5.3). The carbon environment (a hydrocarbon gas) is used to set the surface-carbon content ( $c_s$ ) at 1.0 wt %. The initial carbon content of the steel ( $c_0$ ) is 0.2 wt %. Using the error-function table, calculate how long it would take at 1,000°C to reach a carbon content of 0.6 wt % [i.e.,  $(c - c_0)/(c_s - c_0) = 0.5$ ] at a distance of 1 mm from the surface.

**SOLUTION**

Using Equation 5.11, we get

$$\frac{c_x - c_0}{c_s - c_0} = 0.5 = 1 - \operatorname{erf}\left(\frac{x}{2\sqrt{Dt}}\right)$$

or

$$\operatorname{erf}\left(\frac{x}{2\sqrt{Dt}}\right) = 1 - 0.5 = 0.5.$$

Interpolating from Table 5.1 gives

$$\frac{0.5 - 0.4755}{0.5205 - 0.4755} = \frac{z - 0.45}{0.50 - 0.45}$$

or

$$z = \frac{x}{2\sqrt{Dt}} = 0.4772$$

or

$$t = \frac{x^2}{4(0.4772)^2 D}.$$

Using the diffusivity calculation from Example 5.3, we obtain

$$\begin{aligned} t &= \frac{(1 \times 10^{-3} \text{ m})^2}{4(0.4772)^2 (2.98 \times 10^{-11} \text{ m}^2/\text{s})} \\ &= 3.68 \times 10^4 \text{ s} \times \frac{1 \text{ h}}{3.6 \times 10^3 \text{ s}} \\ &= 10.2 \text{ h.} \end{aligned}$$

**EXAMPLE 5.5**

Recalculate the carburization time for the conditions of Example 5.4 using the master plot of Figure 5.11 rather than the error-function table.

**SOLUTION**

From Figure 5.11, we see that the condition for  $(c - c_0)/(c_s - c_0) = 0.5$  is

$$\frac{x}{\sqrt{Dt}} \approx 0.95$$

or

$$t = \frac{x^2}{(0.95)^2 D}$$

Using the diffusivity calculation from Example 5.3, we obtain

$$\begin{aligned} t &= \frac{(1 \times 10^{-3} \text{m})^2}{(0.95)^2 (2.98 \times 10^{-11} \text{m}^2/\text{s})} \\ &= 3.72 \times 10^4 \text{s} \times \frac{1 \text{ h}}{3.6 \times 10^3 \text{s}} \\ &= 10.3 \text{ h.} \end{aligned}$$

**Note.** There is appropriately close agreement with the calculation of Example 5.4. Exact agreement is hindered by the need for graphical interpretation (in this problem) and tabular interpolation (in the previous problem).

**EXAMPLE 5.6**

For a carburization process similar to that in Example 5.5, a carbon content of 0.6 wt % is reached at 0.75 mm from the surface after 10 h. What is the carburization temperature? (Assume, as before, that  $c_s = 1.0$  wt % and  $c_0 = 0.2$  wt %.)

**SOLUTION**

As in Example 5.5,

$$\frac{x}{\sqrt{Dt}} \approx 0.95$$

or

$$D = \frac{x^2}{(0.95)^2 t}$$

with the following data given:

$$D = \frac{(0.75 \times 10^{-3} \text{m})^2}{(0.95)^2 (3.6 \times 10^4 \text{s})} = 1.73 \times 10^{-11} \text{m}^2/\text{s}.$$